Available online at www.sciencedirect.com

SCIENCE DIRECT

Journal of Nutritional Biochemistry 17 (2006) 548–560

Journal of Nutritional Biochemistry

Compendium of the antidiabetic effects of supranutritional selenate doses. In vivo and in vitro investigations with type II diabetic *db/db* mice

Andreas S. Mueller, Josef Pallauf*

Institute of Animal Nutrition and Nutritional Physiology, Justus Liebig University Giessen, D-35392 Giessen, Germany

Received 23 August 2005; received in revised form 14 October 2005; accepted 15 October 2005

Abstract

In recent years, a number of investigations on the antidiabetic effects of supranutritional selenate doses have been carried out. Selenate (selenium oxidation state +VI) was shown to possess regulatory effects on glycolysis, gluconeogenesis and fatty acid metabolism, metabolic pathways which are disturbed in diabetic disorders. An enhanced phosphorylation of single components of the insulin signalling pathway could be shown to be one molecular mechanism responsible for the insulinomimetic properties of selenate. In type II diabetic animals, a reduction of insulin resistance could be shown as an outcome of selenate treatment. The present study with *db/db* mice was performed to investigate the antidiabetic mechanisms of selenate in type II diabetic animals.

Twenty-one young adult female *db/db* mice were randomly assigned to three experimental groups (selenium deficient=0Se, selenite-treated group=SeIV and selenate-treated group=SeVI) with seven animals each. Mice of all groups were fed a selenium-deficient diet for 8 weeks. The animals of the groups SeIV and SeVI were supplemented with increasing amounts of sodium selenite or sodium selenate up to 35% of the LD_{50} in week 8 in addition to the diet by tube feeding.

Selenate treatment reduced insulin resistance significantly and reduced the activity of liver cytosolic protein tyrosine phosphatases (PTPs) as negative regulators of insulin signalling by about 50%. In an in vitro inhibition test selenate (oxidation state +VI) per se did not inhibit PTP activity. In this test, however, selenium compounds of the oxidation state +IV were found to be the actual inhibitors of PTP activity.

Selenate administration in vivo further led to characteristic changes in the selenium-dependent redox system, which could be mimicked in an in vitro assay and provided further evidence for the intermediary formation of SeIV metabolites. The expression of peroxisome proliferator-activated receptor gamma (PPARγ), another important factor in the context of insulin resistance and lipid metabolism, was significantly increased by selenate application. In particular, liver gluconeogenesis and lipid metabolism were influenced strongly by selenate treatment.

In conclusion, our results showed that supranutritional selenate doses influenced two important mechanisms involved in insulin-resistant diabetes, namely, PTPs and PPARγ, which, in turn, can be assumed as being responsible for the changes in intermediary metabolism, e.g., gluconeogenesis and lipid metabolism. The initiation of these mechanisms thereby seems to be coupled to the intermediary formation of the selenium oxidation state +IV (selenite state) from selenate.

Keywords: Antidiabetic effects; Selenate; Protein tyrosine phosphatase

1. Introduction

When taken up at the recommended level (animals: 0.15–0.30 mg Se/kg dietary dry matter; humans: 50–70 μg Se daily), selenium performs its physiological functions in the body of animals and humans as an integral part of the redox-active centre of functional selenoproteins [1–5]. The detoxification of peroxides, the involvement in the regulation of thyroid hormone metabolism and the participation in the reduction of disulfides and ascorbate are the most important functions fulfilled by the functional selenoproteins, glutathione peroxidase, iodothyronine deiodinase and thioredoxin reductase [6–8].

In human food, selenium is present in two major forms. Feedstuffs derived from animal sources mainly contain selenium in the form of selenocysteine from functional selenoproteins, whereas selenium from plant-derived foodstuffs is present predominantly as selenomethionine. In

* Corresponding author. Tel.: +49 641 9939231; fax: +49 641 9939239.
E-mail address: josef.pallauf@ernaehrung.uni-giessen.de (J. Pallauf).

0955-2863/$ – see front matter © 2006 Elsevier Inc. All rights reserved.
doi:10.1016/j.jnutbio.2005.10.006

trace element supplements, selenium is frequently added in the form of inorganic salt, sodium selenite (selenium oxidation state +IV and sodium selenate +VI). Selenium from various dietary sources is absorbed in the jejunum and in the ileum of mammals. The amino acid derivatives selenomethionine and selenocysteine use the same carriers as their sulphur analogues methionine and cysteine [9]. Selenate uses a sodium-sulphate cotransporter for its absorption, which is driven by the activity of Na^+/K^+-ATPase at the basolateral enterocyte membrane [10]. In contrast, selenite prior to its absorption partially reacts with glutathione and other thiols in the lumen to form selenotrisulfides, which are presumably taken up into the enterocytes by amino acid transporters. Another part of selenite diffuses through the apical membrane and reacts with thiols in the cytosol of enterocytes [10]. The selenium compounds mentioned above are absorbed, to a high extent (> 85%), from dietary sources, but differences exist in the absorption time. As a result of the upstream selenotrisulfide synthesis, selenite absorption is slower than selenate and selenomethionine absorption [10]. Subsequently, the selenocompounds are released into the blood stream at the basolateral enterocyte membrane and distributed to the various peripheral tissues. The exact transport mechanism for the various selenium compounds is not fully understood yet. Selenomethionine associates with hemoglobin, while selenate and the remaining free selenite were found to be transported with α- and γ-globulins [11,12]. Thus, orally administered selenite presumably enters the peripheral organs in the form of selenotrisulfides, or it is reduced in the erythrocytes. Selenate is metabolised during and after its unmodified uptake by the peripheral tissues (Fig. 1).

This hypothesis of a distinctly different cellular metabolism for selenite and selenate is supported by an investigation into intermediary selenium metabolites after intravenous injection of rats with both compounds [13,14]. Selenite was rapidly taken up by red blood cells, reduced in the erythrocytes to the selenide oxidation state −II and delivered to peripheral organs (liver) in an albumin-bound form. In contrast, unmodified selenate could be detected in the bloodstream, and the successive reduction to the oxidation state −II takes place during selenate uptake from plasma to peripheral organs. A fraction of "acid labile selenium" consisting of selenium bound unspecifically to proteins (presumably via the formation of Se-S bonds) could be detected. After intravenous injection with both compounds, the main excretion products detected in urine consisted of the methylated forms of selenium (monomethylselenol and trimethylselenonium ion). Injection of selenite (SeIV) led to a major peak of these methylated metabolites in urine after 0–6 h in comparison to a selenate (SeVI) injection, which showed high metabolite concentrations after 6–12 h. Additionally, unmodified selenate was excreted after selenate injection [14].

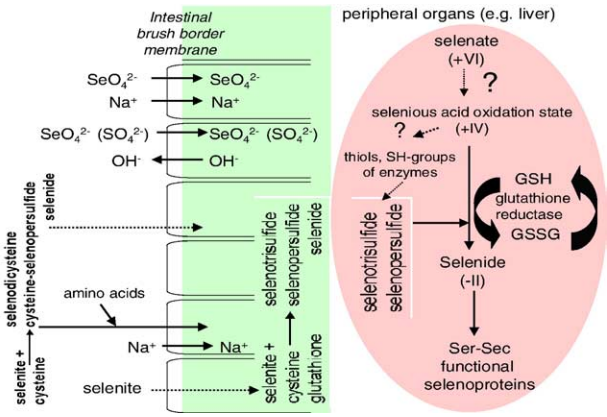

Fig. 1. Current comprehension of mammalian selenium absorption and metabolism.

Selenomethionine is the only selenium compound that can be incorporated unspecifically into proteins instead of its sulphur analogue methionine. The ongoing cellular metabolism of all selenium compounds requires a step-by-step glutathione-dependent reduction to the selenide oxidation state −II, which is the physiological basis for the incorporation of the trace element into the selenocysteine residue of functional selenoproteins by a cotranslational mechanism [15–17].

In recent years, a fascinating new physiological aspect has been found for selenate. Selenate administration in supranutritive doses (daily administration of amounts up to the individual LD_{50} for about 8 weeks) to rats with streptocotozin-induced type I diabetes led to a sustained correction of their diabetic status including the decrease of the elevated blood glucose concentration and considerable changes in the expression of abnormally expressed glycolytic and gluconeogenic marker enzymes [18–24]. From in vivo experiments and in vitro studies with tissue cultures, it was concluded that enhanced phosphorylation reactions at the β subunit of the insulin receptor and further components of the insulin signalling cascade are responsible for the so-called insulinomimetic properties of selenate [25,26].

Oral treatment of mice with alloxan-induced type I diabetes with a high dose of selenite (4 mg/kg body weight per day) failed to reduce hyperglycemia in these animals, which seems to be based on differences in the intermediary metabolism of selenite and selenate [27].

Insulinomimetic properties of selenate could also be found in type II diabetic *db/db* mice. In this animal model featuring severe symptoms of type II diabetes [28,29], the antidiabetic effect of selenate could be attributed to the reduction of insulin resistance, whereas the in vivo administration of selenite did not result in a significant amelioration of insulin resistance and diabetes [28].

Besides the influence of insulin and therefore of insulin sensitising agents on glucose metabolism, hormones also play a crucial role in fatty acid metabolism.

Peroxisome proliferator-activated receptors (PPARs) are originally transcription factors belonging to the superfamily of nuclear receptors, discussed as acting as master regulators of fatty acid metabolism and displaying an important link between fatty acid metabolism and insulin sensitivity. Three isoforms (α, β and γ) have been described. They act on DNA response elements as heterodimers with the nuclear retinoic acid receptor. Their natural activating ligands are fatty acids and lipid-derived substrates. PPARα is present predominantly in the liver and heart and, to a lesser extent, in skeletal muscle. When activated, it promotes fatty acid oxidation, ketone body synthesis and glucose sparing. Peroxisome proliferator-activated receptor gamma (PPARγ) is considered to be one of the master regulators of adipocyte differentiation. The isoform PPARγ2 is abundantly expressed in mature adipocytes and is elevated in animals with fatty livers.

Thiazolidinediones were developed as antidiabetic drugs acting as synthetic ligands of PPARs. They increase peripheral glucose utilisation and reduce insulin resistance [30,31]. The whole complex of tissue-specific actions and interactions of PPARs is not yet fully understood. In a study with transgenic mice, animals without liver PPARγ but with adipose tissue developed fat intolerance, increased adiposity, hyperlipidemia and insulin resistance. Thus, it was concluded that liver PPARγ regulates triglyceride homeostasis, contributing to hepatic steatosis, but protecting other tissues from triglyceride accumulation and insulin resistance [32,33]. Moreover, it was shown that the treatment of *db/db* mice with thiazolidinediones induced expression in the liver of adipose tissue PPARγ target genes, such as adipocyte FABP [34], which foretells that hepatic lipid accumulation (steatosis) could occur during long-term administration [35,36].

The present study with young female *db/db* mice was therefore carried out to investigate the mechanisms by which selenate influences insulin resistance and metabolic pathways in type II diabetic mice.

2. Materials and methods

2.1. Animals and diets

Twenty-one young female *db/db* mice (C57BL/KsOlaHsd-Leprdb) aged 6 weeks with an average body weight of 43.7±2.03 g were obtained from Harlan/Winkelmann (Borchen, Germany). The animals had previously been fed a standard chow for mice containing 0.25 mg selenium as sodium selenite per kilogram diet. The mice were randomly assigned to three groups of seven animals each (selenium deficient=0Se, selenite-treated group=SeIV and selenate-treated group=SeVI) and individually housed in plastic cages with shavings as bedding material at 22°C room temperature and a 12:12-h light/dark cycle. The animals of all groups were fed a selenium-deficient experimental diet (<0.02 mg Se/kg diet) based on torula yeast (Table 1).

With the exception of Se, the diet was formulated to meet the current recommendations for mice [1]. Mice of the group 0Se were kept on a selenium-deficient diet for 8 weeks. The animals of groups SeIV and SeVI were supplemented with amounts increasing from 15% up to 35% of the LD_{50} of sodium selenite and sodium selenate by week 8 in addition to the diet by tube feeding (LD_{50} of sodium selenite and sodium selenate ~3.5 mg/kg body weight).

After 2 days of recovery from the final insulin resistance test (IRT), the mice of all experimental groups were anaesthetised in a carbon dioxide atmosphere and subsequently decapitated. Organs were immediately removed, frozen in liquid nitrogen and stored at −80°C until analysis. Small pieces from all organs were placed in RNA later and frozen at −20°C for RNA extraction.

The protocol of the animal experiment was approved by the regional council of Giessen.

2.2. Performance of a whole-body insulin sensitivity test

Before subjecting the mice to the specified dietary conditions (initial status) and after 8 weeks under experimental conditions, their whole-body insulin resistance was evaluated.

Insulin sensitivity tests (ISTs) in mice fasted overnight were performed by subcutaneous injection of 2 IU insulin/kg body weight (Insuman Infusat 100 IU/ml from AVENTIS Pharma Deutschland, Frankfurt/Main, Germany). Glucose concentration in blood sampled from

Table 1
Composition of the selenium-deficient basal diet, based on torula yeast

Dietary components	Content (g/kg diet)
Torula yeast	300.0
Cellulose BWW 40	50.0
Soybean oil	25.0
Coconut oil	25.0
DL-Methionine	3.0
Premix of minerals and trace elements (without selenium)[a]	66.6
Premix of vitamins[b]	10.0
Choline chloride	2.0
Wheat (low in selenium)	450.0
Maize starch	68.4
Total	1000

[a] Minerals and trace elements added per kg diet: $CaCO_3$: 12.5 g=5.090 mg Ca/kg diet; KH_2PO_4: 15.0 g=2.650 mg P/kg diet; Na_2HPO_4: 7.5 g=1.630 mg P/kg diet; $MgSO_4 \times 7\ H_2O$: 5.0 g=508 mg Mg/kg diet; NaCl: 4.0 g=1.56 g Na/kg diet; $CuSO_4 \times 5\ H_2O$: 20 mg=5.10 mg Cu/kg diet; $FeSO_4 \times 7\ H_2O$: 250 mg=50.2 mg Fe/kg diet; $ZnSO_4 \times 7\ H_2O$: 150 mg=34.1 mg Zn/kg diet; $MnSO_4 \times H_2O$: 130 mg=47.4 mg Mn/kg diet; $CrCl_3$: 7.5 mg=2.47 mg Cr/kg diet; NaF: 2.2 mg=0.99 mg F/kg diet; KJ: 0.3 mg=0.23 mg J/kg diet; $CoSO_4 \times 7\ H_2O$: 1.2 mg=0.25 mg Co/kg diet; $Na_2MoO_4 \times 2\ H_2O$: 0.5 mg=0.20 mg Mo/kg diet.

[b] Vitamins added per kilogram diet: vitamin A: 15000 IU; vitamin D: 1500 IU; vitamin E: 15 IU; vitamin K_3: 5 mg; vitamin B_1: 10 mg; vitamin B_2: 10 mg; vitamin B_6: 10 mg; vitamin B_{12}: 0.02 mg; niacin: 50 mg; pantothenic acid: 10 mg; biotin: 0.3 mg; vitamin C: 150 mg.

the tail vein was recorded before starting the test and 30, 60, 90, 120, 180, 240 and 300 min after insulin injection. Blood glucose concentration during IRT was determined using a glucometer (Bayer Elite).

The protocol of the animal experiment was approved by the regional council of Giessen.

2.3. Determination of biochemical and physiological parameters

2.3.1. Measurement of parameters of the selenium-dependent redox system in the liver

2.3.1.1. Glutathione peroxidase 1 and test of the influence of different selenium compounds on GPx1 activity in vitro. Glutathione peroxidase 1 was measured in the cytosol of 1:10 (w/v) liver homogenates by the indirect spectrophotometric procedure coupled to glutathione reductase [37]. NADPH oxidation was recorded for 3 min at 340 nm. A blank without added liver cytosol was carried out for each sample. The activity of GPx1 was calculated from the absorption difference. One unit of GPx1 was defined as 1 μmol NADPH oxidized per minute under the described conditions. The activity of GPx1 was normalized to 1 mg protein.

To test the influence of the inorganic selenium compounds selenate (oxidation state +VI) and selenite (oxidation state +IV) on the glutathione peroxidase and glutathione reductase–redox system, final selenium concentrations of up to 1000 μmol/L as selenate and selenite were added to the glutathione peroxidase assay (which contains all components of the glutathione peroxidase redox system: reduced glutathione, glutathione reductase, NADPH and glutathione peroxidase from the sample) as described above, replacing 10 μl of the assay buffer by selenate and selenite dissolved in bidistilled water.

2.3.1.2. Glutathione reductase. The activity of glutathione reductase in the liver of the *db/db* mice was determined using a standard procedure that is coupled to NADPH oxidation [38].

2.3.1.3. Total glutathione and oxidized glutathione. The concentration of total glutathione and oxidized glutathione was analysed according to the standard protocol coupled to glutathione reductase and DTNB [39]. Sample concentrations were calculated from a standard curve prepared with pure glutathione disulfide (GSSG) (concentration range: 0–0.066 μmol GSSG/ml).

2.3.1.4. Thioredoxin reductase. The activity of thioredoxin reductase was determined by the NADPH and DTNB-coupled procedure [40]. Prior to the measurement of thioredoxin reductase activity, the 1:10 (w/v) liver homogenates were dialysed against PBS in order to remove the interfering glutathione. DTNB reduction was measured for 3 min at 412 nm. One unit of thioredoxin reductase activity was defined as 1 μmol DTNB reduced per minute. Enzyme activity was normalised to 1 mg protein.

2.3.2. Determination of the activity of cytosolic protein tyrosine phosphatases (PTPs) in the liver and assay of the "*in vitro inhibition*" of PTPs by different selenium compounds

Protein tyrosine phosphatase activity was determined with modifications according to a method based on the hydrolysis of paranitrophenyl phosphate (pNPP) [41,42] as published earlier. The inhibition of PTP activity by different selenium compounds was developed using pooled liver cytosol from three adult female *db/db* mice fed a standard chow containing 0.25 mg Se/kg diet.

The activity of PTPs was assessed as described above for liver homogenates obtained from the in vivo trial. In addition to the above procedure, 10 μl of aqueous solutions of sodium selenate (oxidation state: +VI), nonenzymatically reduced selenate (using 37% HCl as the reducing agent; oxidation state: +IV), sodium selenite (oxidation state: +IV), selenious acid (oxidation state: +IV) and freshly synthesized selenotrisulfides from the reaction of reduced glutathione and selenite in a molar ratio of 4:1 (synthesized according to a standard protocol [43]; oxidation state: +II), reaching final selenium concentrations of 25–5000 μmol/L, were added before incubation of the reaction mixtures with pNPP for 10 min. A blank without cytosol was carried out for all determinations. The inhibition of PTPs was expressed as the percent inhibition in comparison with the PTP activity obtained in liver cytosol without addition of selenium compounds.

2.3.3. RT-PCR analysis to examine the expression of protein tyrosine phosphatase 1B (PTP1B), PPARγ, fructose-1,6-diphosphatase (F-1,6-Dptase) and phosphoenolpyruvate carboxykinase (PEPCK)

For the RT-PCR analysis of PTP1B expression in the liver, total RNA was prepared using the acid guanidinium thiocyanate extraction method as described previously [44]. The extracted RNA was dissolved in DEPC-treated water, and the concentration and purity were determined in an UV visible photometer at 260 and 280 nm. To check the quality of the RNA preparations, 10 μg of total RNA from each preparation was separated electrophoretically in 1.5% formaldehyde containing agarose gels. The RNA solutions were diluted with DEPC-treated water to a final concentration of 2 μg/μl. From the diluted RNA solutions for each experimental group (0Se, SeIV and SeVI), three RNA pools from two animals were prepared. Five micrograms (2.5 μl) of the RNA pools was used for reverse transcription with a cDNA synthesis kit (RevertAID H Minus First Strand cDNA Synthesis Kit, #K1631 from MBI Fermentas). For this purpose, the procedure using the oligo (dT_{18}) primers was chosen. The cDNA was diluted 1:3 with DEPC-treated water. The use of 2 μl of this diluted cDNA for the amplification of gene-specific fragments was optimal to obtain the linear range of amplification.

Gene	Length of amplificate	Forward and reverse primer	Annealing temperature	Number of amplification cycles (*x* times)
PTP1B	701	5′-GAT GGA GAA GGA GTT CGA GGA G-3′ 5′-CCA TCA GTA AGA GGC AGG TGT C-3′	59.2	30
PPARγ	348	5′-GAG TCT GTG GGG ATA AAG CAT C-3′ 5′-CTC CAG GAC TCC TGC ACA T-3′	57.6	31
PEPCK	700	5′-AGC CTT TGG TCA ACA ACT GG-3′ 5′-CTA CGG CCA CCA AAG ATG AT-3′	54.3	27
F-1, 6-Dptase	447	5′-GTC AAC TGC TTC ATG CTG GA-3′ 5′-CCA CCA CCC TGT TGC TGT AG-3′	57.0	26
GAPDH	303	5′-ACG GGA AGC TCA CTG GCA TG-3′ 5′-CCA CCA CCC TGT TGC TGT AG-3′	cf. gene-specific temperatures	26

The PCR reactions for the amplification of fragments from the coding sequence of the genes examined were carried out in a reaction volume of 50 μl with a standard program for the single cycles. The standard program was as follows: initial denaturation: (95°C, 3 min) 1×; amplification cycles: (denaturation: 95°C, 45 s; annealing: primer-specific temperature, 40 s; extension: 72°C, 55 s) *x* times; final extension: (72°C, 5 min) 1×.

The further conditions in a typical 50-μl reaction were as follows:

10× PCR buffer (20 mM MgCL from MBI Fermentas)	5.00 μl
Taq Polymerase (Invitek)	0.04 U/μl
Mixed dNTPs (2 mM)	3.80 μl
Primer forward (10 pmol/μl)	2.50 μl
Primer reverse (10 pmol/μl)	2.50 μl
Nuclease free water	36.20 μl

The GAPDH fragment was amplified for 26 cycles.

Six microlitres of the amplification products was separated by electrophoresis in 1.5% agarose gels containing 0.1 μg ethidium bromide per millilitre. A molecular weight marker (Gene Ruler 100-bp DNA Ladder Plus #SM0321 from MBI Fermentas) was carried along in the gels. Additionally, the expression of the abovementioned genes was also examined in RNA samples obtained from three age- and sex-matched nondiabetic Black 6 mice. The gels were photographed under UV light with a gel imager (Gene Flash from Syngene), and optical density was evaluated using the software for the Syngene Imager. The expression of the genes examined was normalised to GAPDH expression.

2.3.4. Determination of the gluconeogenic marker enzymes F-1,6-Dptase, pyruvate carboxylase, phosphoenolpyruvate caboxykinase

The activity of the gluconeogenic marker enzymes F-1,6-Dptase, pyruvate carboxylase (PC) and PEPCK was measured photometrically by standard assays coupled to NAD/NADP–NADH/NADPH [45–47].

2.3.5. Measurement of parameters of lipid metabolism

2.3.5.1. Extraction of crude lipids from the liver. For the extraction of crude lipids, firstly, 1:10 (w/v) homogenates were prepared in 0.154 mol/L NaCl under a N_2 atmosphere using 0.25 g of liver per sample. To each sample, 2.5 ml of a hexane/isopropanol (3:2) mixture containing 0.005% butylated hydroxytoluene was then added. The samples were vortexed for 1 min and incubated at room temperature for 1 h after gassing with N_2. After centrifugation at 4500 U/min for 15 min, the upper lipid-containing phase was collected in a dried and tared sealable glass tube. The remaining pellet and the lower aqueous phase were then extracted for a further hour using 2 ml of the hexane/isopropanol (3:2) mixture. After centrifugation at 4500 U/min for 15 min, the upper phase was also collected into the first lipid extract. Then the solvent was evaporated in a N_2 atmosphere at 45°C, and, finally, the samples were dried in a vacuum dryer for 2 h.

Lipid concentration was determined gravimetrically, and the lipids were resolved in 1 ml hexane and frozen at −20°C until further analysis.

2.3.5.2. Determination of triglyceride concentration in plasma and liver. The concentration of triglycerides in plasma and in liver lipid extracts was determined with a test kit (Fluitest TG) from Biocon (Bangalore, India). The accuracy of the method was checked with Qualitrol.

2.3.5.3. Determination of cholesterol concentration in plasma and liver lipid extracts. Cholesterol concentration in plasma and in liver lipid extracts was measured with a test kit (Fluitest CHOL) from Biocon (Bangalore, India). The accuracy of the method was checked with Qualitrol.

2.3.5.4. Determination of phospholipid concentration in the liver. The concentration of phospholipids in liver lipid extracts was measured with a test kit from Boehringer (Mannheim, Germany) after digestion of the samples and liberation of the phospholipid phosphorus in a mixture of 70% perchloric acid and 30% H_2O_2.

2.3.6. Determination of the protein concentration in liver homogenates

The protein content in liver homogenates was determined using a standard protocol [48].

2.3.7. Statistical analysis

Statistical analysis of the experimental data was performed using the statistical package SPSS 12.0 for Windows. A one-way analysis of variance was performed after ascertaining the normality of distribution (Kolmogorov–Smirnov test or Shapiro–Wilk test) and the homogeneity of variance (Levene test) of the experimental data. If both conditions were fulfilled, differences between means were evaluated using the Tukey test. If homogeneity of variance could not be ensured, differences between means were examined using the Dunnett T3 test. Differences between means were assumed as significant at an error probability of less than 5% ($P<.05$). For some results, a trend is shown when error probability was less than 10% ($P<.1$).

3. Results

3.1. Whole-body insulin sensitivity

Fig. 2 shows the results of the whole-body IST. The blood glucose concentrations after the insulin challenge in the experimental groups are given as a percentage obtained in the initial status before putting the mice on special dietary conditions. Selenate treatment kept insulin sensitivity at a comparable level as in the initial status.

In selenium-deficient mice, initial blood glucose concentration (time: 0 min) before insulin injection was 1.5 to 2 times higher than in the initial status and in the selenate-treated mice. The lowering of blood glucose concentration in these groups takes place at significantly higher mean blood glucose concentrations. The higher insulin resistance in selenium-deficient and selenite-treated mice is indicated by a steep rise in the blood glucose response curve towards the initial values after 120 min.

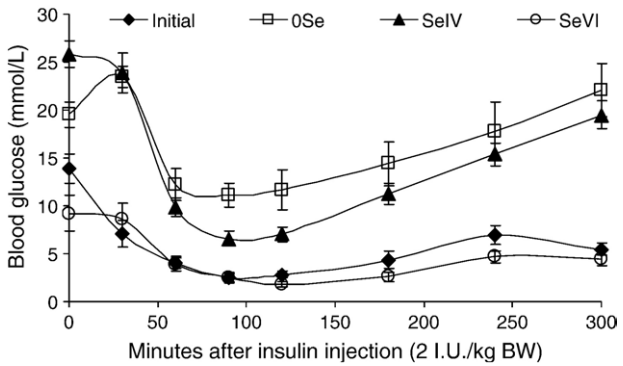

Fig. 2. Whole-body insulin sensitivity of *db/db* mice treated with selenate for 8 weeks in comparison to selenium-deficient and selenite-treated mice and to their initial status, obtained before putting the mice on defined dietary conditions. Each data point represents the mean±S.E.M. of seven animals per group.

Table 2
Parameters of the selenium- and glutathione-dependent cellular redox system: glutathione peroxidase 1 (mU/mg protein), thioredoxin reductase (mU/mg protein), glutathione reductase (mU/mg protein) and concentrations of total, oxidized and reduced glutathione in the liver of *db/db* mice treated with selenate for 8 weeks in comparison to selenium-deficient mice and selenite-treated mice (mean±S.D.)

Parameter of the selenium-and glutathione-dependent antioxidative system	0Se	SeIV	SeVI
Glutathione peroxidase 1	171 ± 25.9^{a}	703 ± 150^{c}	369 ± 43.1^{b}
Glutathione reductase	21.3 ± 2.27^{a}	17.2 ± 1.86^{a}	25.6 ± 4.54^{b}
Thioredoxin reductase	17.2 ± 9.77^{a}	53.1 ± 9.71^{b}	76.9 ± 24.9^{b}
Total glutathione	5.50 ± 0.49^{a}	6.69 ± 0.81^{b}	$6.24\pm0.97^{ab(<0.1)}$
Reduced glutathione	2.64 ± 0.32^{b}	2.13 ± 0.51^{a}	2.37 ± 0.51^{ab}
Oxidized glutathione	2.85 ± 0.27^{a}	4.56 ± 0.58^{b}	3.87 ± 0.49^{b}
% Reduced of total	48.03	31.67	37.71
% Oxidized of total	51.97	68.33	62.29

Significant differences ($P<.05$) within a row are indicated by different superscripts, "(<0.1)" shows a trend; $n=7$ animals per group considered for glutathione peroxidase and glutathione reductase; $n=6$ animals per group considered for glutathione- and thioredoxin reductase.

3.2. Selenium- and glutathione-dependent redox system

Eight weeks of supranutritional supplementation with selenite and selenate resulted in a significantly higher activity of liver GPx1 in selenite-treated and selenate-treated mice than in selenium-deficient mice. Thereby, it is noticeable that the selenate-treated mice had a significantly lower GPx1 activity than the mice with selenite application (Table 2).

The activity of both glutathione- and thioredoxin reductase was significantly increased by selenate treatment in comparison to the two other groups. With regard to the glutathione redox pair, the following measurements were made. Total glutathione concentration was slightly increased in the livers of both selenium-treated groups in comparison to the selenium-deficient group. This effect was significant between the selenite-treated group and the selenium-deficient group and in tendency between selenate-treated mice and selenium-deficient animals. The concentration of oxidized glutathione and the ratio of oxidized to total glutathione were increased by selenium treatment with both selenite and selenate; thus, the glutathione redox pair shifted to a more oxidized state. An attempt to mimic these characteristic changes of glutathione peroxidase and glutathione reductase activity in selenate-treated mice was made in vitro. As also found in the in vitro inhibition assay for PTPs (cf. Section 4.2), this in vitro assay provided evidence that in the intermediary metabolism of selenium compounds

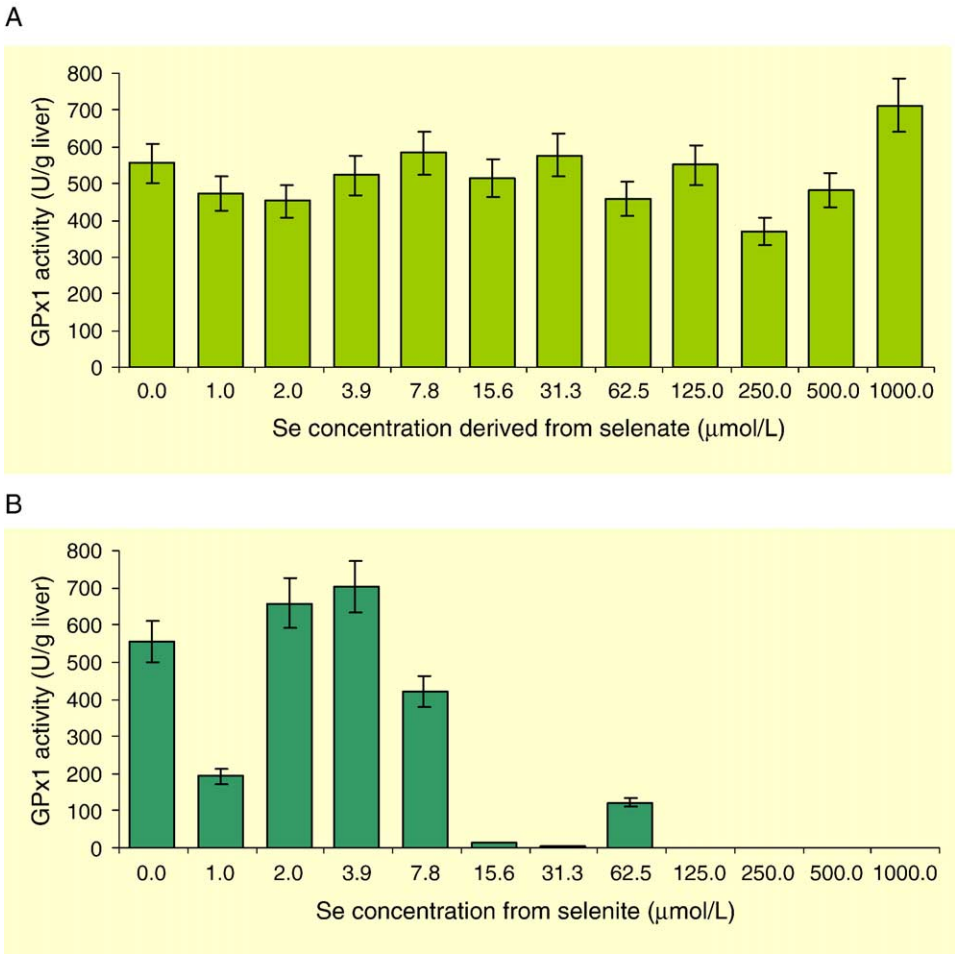

Fig. 3. Influence of different selenate (A) and selenite concentrations (B) on glutathione peroxidase activity in vitro. Each bar represents the mean±S.D. of three independent replications.

the selenite oxidation state +IV must be formed from selenate (oxidation state +VI) and is the actual biologically active metabolite.

The addition of increasing concentrations of selenate (0–1000 μmol/L) to the glutathione peroxidase assay (containing all components of the glutathione-dependent

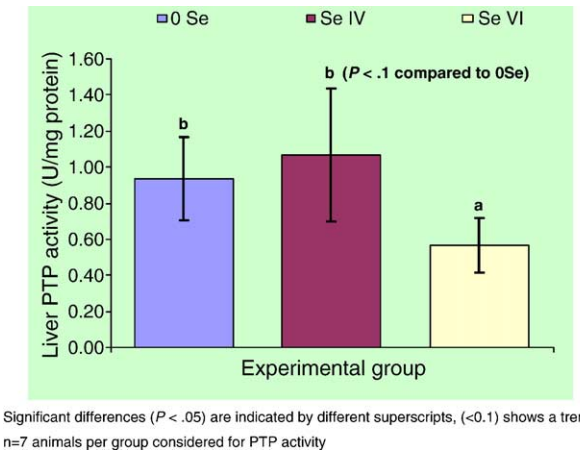

Fig. 4. Effect of 8 weeks of selenate treatment (SeVI) on the activity of PTPs (mean±S.D.) in the liver of *db/db* mice in comparison to selenium-deficient mice and selenite-treated mice.

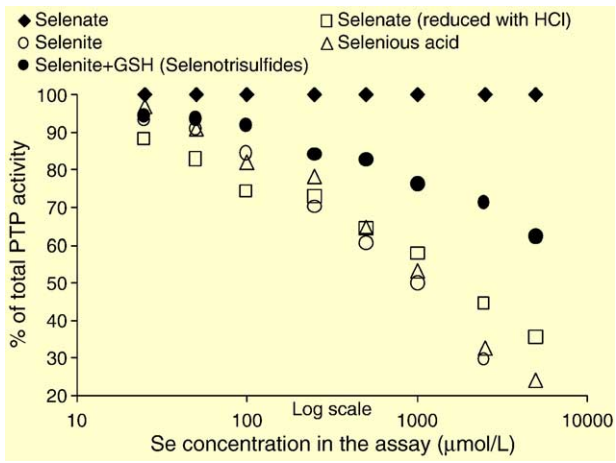

Fig. 5. In vitro test on the inhibition of PTPs by different selenium compounds and concentrations. Each data point represents the mean of three independent replications.

redox system) showed no overall influence on the activity of glutathione peroxidase activity (Fig. 3A). In contrast, the addition of selenite led to a reduction of glutathione peroxidase activity while the blank activity (glutathione reductase-dependent NADPH activity) increased. The addition of selenite concentrations above 62.5 μmol/L led to a total breakdown of the reaction (Fig. 3B).

3.3. Activity of PTPs as important antagonists of insulin signaling

Selenate treatment for 8 weeks inhibited the activity of PTPs as important antagonists of insulin signalling by about 50% as compared to selenium-deficient and selenite-treated animals (Fig. 4).

To ascertain the inhibitory effect of selenium compounds in different oxidation states on the activity of PTPs, an in vitro inhibition test was performed.

The addition of selenate (selenium oxidation state: +VI) to the reaction mixture reaching final selenium concentrations of 25, 50, 100, 250, 500, 1000, 2500 and 5000 μmol/L produced no inhibition of PTP activity. Adding selenium compounds of the oxidation state +IV, obtained either by nonenzymatic reduction of selenate with 37% HCl or by the addition of pure selenite or selenious acid to the reaction mixture, led to a strong inhibition of PTPs in a concentration-dependent manner (Fig. 5). A 50% inhibition of PTP activity was obtained with all the abovementioned selenium compounds of the oxidation state +IV when their final concentration in the assay mixture ranged between 500 and 1000 μmol/L. The inhibition of PTPs by tetravalent selenium compounds steadily increased up to the highest concentration examined in the test (5000 μmol/L Se), reaching a 65% inhibition by nonenzymatically reduced selenate and an 85% and 76% inhibition by the addition of pure selenite and selenious acid, respectively. Selenotrisulfides (oxidation state: −I), synthesized from selenite and reduced glutathione, effected a significantly lower inhibition of PTPs in comparison with the tetravalent selenium compounds. One hundred, 250, 500 and 1000 μmol/L of selenotrisulfides inhibited PTP activity only by 9%, 17%, 18% and 24%, respectively. Even with the addition of 5000 μmol/L selenotrisulfides to the reaction mixture the inhibition of PTPs remained below 50%.

Table 3
Activity of F-1,6-Dptase (U/mg protein), PC (U/mg protein) and PEPCK (U/mg protein) in the liver of *db/db* mice treated with selenate for 8 weeks in comparison to selenium-deficient and selenite-treated mice (mean±S.D.)

Gluconeogenic marker enzyme	0Se	SeIV	SeVI
Fructose-1,6-Dptase	0.640 ± 0.065^{b}	0.574 ± 0.014^{b}	0.237 ± 0.061^{a}
Pyruvate carboxylase	0.646 ± 0.059^{ab}	0.846 ± 0.220^{b}	0.595 ± 0.045^{a}
Phosphoenolpyruvate carboxykinase	0.306 ± 0.066^{b}	0.261 ± 0.069^{ab}	0.196 ± 0.051^{a}

Significant differences ($P<.05$) within a row are indicated by different superscripts; $n=6$ animals per group considered for the activities of F-1,6-Dptase, PC and PEPCK.

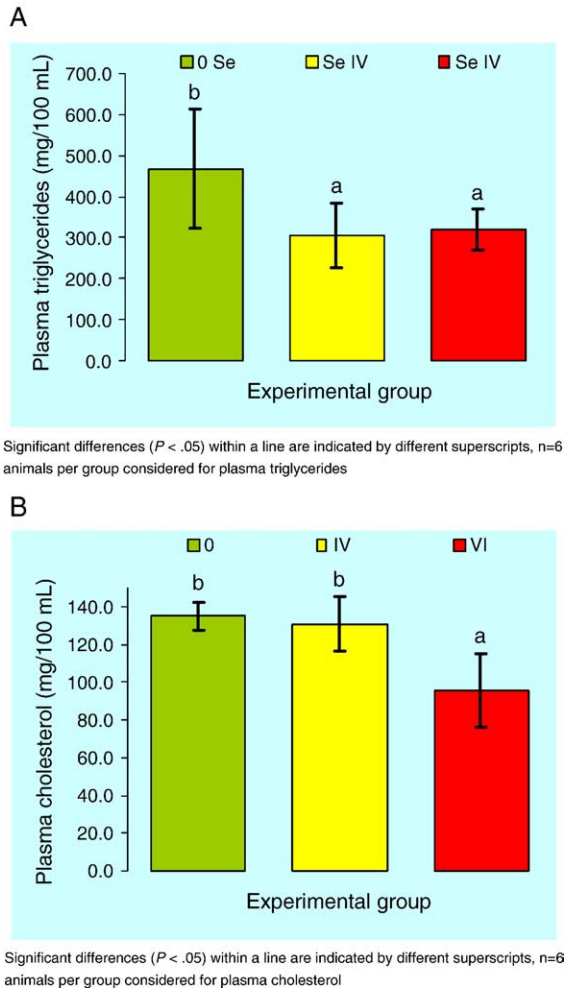

Fig. 6. Triglyceride concentration (mg/100 ml) (A) and cholesterol concentration (mg/100 ml) (B) in plasma of *db/db* mice treated with selenate for 8 weeks in comparison to selenium-deficient and selenite-treated mice (mean±S.D.).

The results of the PTP in vitro inhibition test provided further evidence that selenium compounds of the selenite oxidation state +IV must be formed intermediarily from selenate and actually mediate the biological properties of selenate in vivo.

Selenate administration to *db/db* mice led to a reduction of the activity of the gluconeogenic enzymes F-1,6-Dptase, PC and PEPCK in comparison to selenium-deficient mice and selenite-treated mice (Table 3).

3.4. Parameters of lipid metabolism

In comparison to selenium deficiency, plasma triglyceride concentration was significantly lowered by administration of both selenium compounds to *db/db* mice (Fig. 6A). Selenate treatment additionally lowered plasma cholesterol concentration in comparison to the two other experimental groups (Fig. 6B).

Treatment of *db/db* mice with selenite increased total liver lipid content per gram fresh matter in tendency, whereas treatment with selenate led to a significant increase in total liver lipids as compared to feeding with selenium-deficient diet (Table 4). No changes could be found for the content of phospholipids. A significantly higher cholesterol concentration was evident in selenite-treated mice than in selenium-deficient and selenate-treated mice.

When the lipid parameters were referred to 1 g of total lipids, all parameters measured were significantly lower in selenate-treated mice than in selenium-deficient and selenite-treated animals, whereas the remnant to 1 g of total lipids was significantly increased by selenate treatment, presumably indicating an increased concentration of free fatty acids.

3.5. Expression of genes related to insulin resistance, glucose metabolism and fatty acid metabolism

With regard to expression of genes related to insulin resistance, glucose metabolism and fatty acid metabolism, some marked changes could be measured. Selenium supplementation with selenite or selenate increased the expression of PTP1B, an important tyrosine phosphatase discussed in the context of insulin resistance, by about 2- or 2.5-fold in comparison to selenium deficiency (Fig. 7A). Selenate administration to the *db/db* mice led to a marked down-regulation of the gluconeogenic marker enzymes F-1.6-Dptase and PEPCK in comparison to selenium-deficient and selenite-treated mice. The expression reached a level almost as low as in nondiabetic Black 6 mice. The expression of the PPARγ as an efficient target in the treatment of obesity and insulin resistance, which is mainly expressed in adipose tissue, but also in the liver of obese rodents, was about 2.5-fold increased in the liver of selenate-treated mice in comparison to their selenium-deficient and selenite-treated companions. Under the conditions examined (up to 31 amplification cycles), no expression of PPARγ could be detected in nondiabetic Black 6 mice (Fig. 7B).

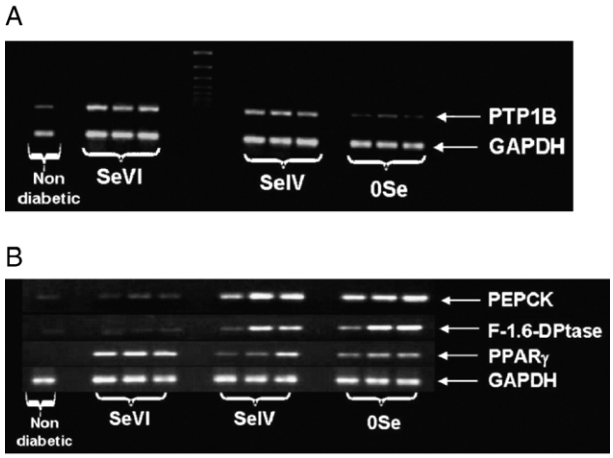

n=6 (3 pools of 2 animals per group) considered for the expression experiments

Fig. 7. Expression of PTP1B (A), PEPCK, F-1.6-Dptase and PPARγ (B) in the liver of *db/db* mice treated with selenate for 8 weeks in comparison to mice on selenium-deficient diet, mice treated with selenite and nondiabetic Black 6 control mice relative to their respective GAPDH expression.

Table 4
Parameters of lipid metabolism: total lipids, triglycerides, phospholipids and cholesterol in the liver of *db/db* mice treated with selenate for 8 weeks in comparison to selenium-deficient mice and selenite-treated mice based on 1 g of liver fresh matter and 1 g of total lipids, respectively (mean±S.D.)

Parameter of liver fatty acid metabolism	0 Se	Se IV	Se VI
Parameters referring to 1 g of liver fresh matter			
Total lipids (mg/g fresh matter)	$79.6\pm7.14^{a(<.1)}$	99.4 ± 16.4^{b}	145 ± 26.9^{c}
Triglycerides (mg/g fresh matter)	36.3 ± 22.1^{a}	$62.7\pm10.6^{b(<.1)}$	$71.0\pm24.0^{b(<.1)}$
Phospholipids (mg/g fresh matter)	18.7 ± 1.19^{a}	18.6 ± 2.16^{a}	19.0 ± 1.32^{a}
Cholesterol (mg/g fresh matter)	3.30 ± 0.64^{a}	4.87 ± 1.00^{b}	3.35 ± 1.13^{a}
Parameters referring to 1 g of liver lipids			
Triglycerides (mg/g lipids)	633 ± 80.9^{a}	639 ± 97.4^{a}	$491\pm150^{b(<.1)}$
Phospholipids (mg/g lipids)	236 ± 20.8^{c}	190 ± 31.5^{b}	138 ± 35.7^{a}
Cholesterol (mg/g lipids)	43.6 ± 7.25^{b}	50.3 ± 11.91^{b}	24.1 ± 10.24^{a}
Rest to 1 g lipids (mg)	87.4	120.7	346.9

Significant differences ($P<.05$) within a row are indicated by different superscripts; "(<0.1)" shows a trend; $n=6$ animals per group considered for liver lipid parameters.

4. Discussion

In the present study, treatment of the *db/db* mice with supranutritional selenate doses effected an improvement of whole-body insulin sensitivity in comparison to selenium-deficient and selenite-treated mice by maintaining insulin sensitivity on a comparably low level as at the beginning of the trial.

4.1. Selenium- and glutathione-dependent redox system

Final GPx1 activity in the liver clearly indicated an efficient selenium depletion in group 0Se. GPx1 activity in the selenium-supplemented groups SeIV and SeVI, on the one hand, reflected a high selenium status in these organs, but, on the other hand, the distinctly lower GPx1 activity in the liver of selenate-treated mice demonstrates that fundamental differences exist in the absorption and the intermediary metabolism of selenite and selenate. The results of the in vitro assay on the influence of selenite and selenate on GPx1 activity strongly suggest that the selenite oxidation state +IV is intermediarily formed from selenate and acts as an inhibitor of GPx1.

Our results with regard to a distinctly different metabolism for selenite and selenate are confirmed by

prior investigations on selenium absorption and by studies characterising intermediary selenium metabolites [9,10,13,14].

From the higher activity of both glutathione reductase and thioredoxin reductase, in particular with selenate treatment, it can be concluded that these reductases are of significance in the reduction of selenate, since selenate must be reduced from the oxidation state +VI to the oxidation state −II, while selenite metabolites (selenotrisulfides) depend only on one reduction step from −I to −II (cf. Fig. 1).

In the present study, the administration of both selenite and selenate further effected a moderate increase in total glutathione concentration and a significant change in the ratio of oxidized to reduced glutathione. Similar findings were reported for a feeding trial with rats and ducklings and could be caused by the enhanced need for reduced glutathione for selenium reduction to the oxidation state −II and a limited capacity of glutathione reductase when supranutritive selenium concentrations are administered to animals [49,50]. Moreover, an increase in oxidized glutathione was reported for rats fed fish oil-enriched diets supplemented with selenium in accordance with dietary recommendations and for rats fed selenium from different compounds in various concentrations [51]. The effects of changes in cellular redox status on insulin resistance have been controversially discussed. On the one hand, a decrease in tissue GSH concentrations by treating rats with the γ-glutamyl cysteinyl synthetase inhibitor buthionine sulfoximine led to a significant impairment of insulin sensitivity of cultured adipocytes from these animals [52]. On the other hand, results from tissue culture studies with α-lipoic acid showed that the short-term enhancement of intracellular oxidant levels led to an enhanced glucose uptake [53]. Further, the effectiveness of pentavalent vanadium, acting as a PTP1B inhibitor on insulin sensitivity, was enhanced in the presence of higher oxidant levels in cells, because under these conditions the reduction of the more effective pentavalent vanadium to less efficient tetravalent vanadium was delayed [54].

4.2. Activity and expression of PTPs as important antagonists of insulin signalling and particular changes in glucose metabolism

A significant decrease of PTP activity in the liver was obtained by oral selenate administration alone. Supranutritional doses of both selenite and selenate increased the expression of PTP1B.

Within the PTPs, a 230-amino acid domain, which includes the active centre of the enzymes, is a highly conserved region in the protein structure. A cysteine residue in this region is involved in the hydrolysis of protein phosphotyrosine residues by the formation of a cysteinyl-phosphate intermediate [55]. In recent years, PTP1B, which is involved in the negative regulation of insulin signalling, has been of particular interest. At present, the expression and activity of PTP1B in rodents and other mammalian species are controversially discussed. However, there is no doubt that diabetic symptoms can be efficiently reduced by treatment with PTP1B enzyme inhibitors or antisense oligonucleotides, which reduce the mRNA expression and the protein synthesis of the enzyme [56–59]. Explanations of the mechanism for reversible and irreversible PTP1B inhibition by glutathionylation in the presence of high concentrations of oxidized glutathione or formation of sulphenic, sulphinic and sulphonic acid derivatives in the presence of hydrogen peroxide have been given involving the blocking as well as the stepwise oxidation of the active site cysteine SH group. Even in vivo, an insulin-dependent release of hydrogen peroxide in tissues leads to an oxidation of PTP1B and an increase in insulin signalling [60–63]. Furthermore, the results of a recent study in mice with GPx1 overexpression support the hypothesis of a differentiated regulation of PTPs by pro- and antioxidative metabolites. In this study, mice with GPx1 overexpression showed a diminished phosphorylation of the β subunit of the insulin receptor [64]. This effect can be explained by a reduced oxidation (inactivation) of the active site of PTPs by reduced hydrogen peroxide levels; thus, the enzymes possess a higher activity towards the phosphorylated β subunit of the insulin receptor, and, therefore, insulin resistance increases. An increased concentration of oxidized glutathione as a result of the increased GPx1 activity, however, may produce higher amounts of glutathionylated PTPs (inactive), leading to an up-regulation of their mRNA and activity, and, finally, effecting an enhanced dephosphorylation of the β subunit of the insulin receptor [64]. From the results of this study and from further unpublished results, we conclude that glutathionylation of PTPs due to a high GPx1 activity and a shift of the glutathione redox pair to a more oxidized state is the driving force for the increased expression of PTP1B.

The in vitro inhibition assay was performed to investigate whether the observed PTP reduction by selenate in vivo is based on the inhibition of these enzymes. Initially, surprisingly and contrary to the in vivo results, the incubation of *db/db* mouse liver cytosol with increasing selenate concentrations (Se oxidation state +VI) effected no inhibition of PTPs, whereas the incubation with SeIV compounds obtained either by nonenzymatic reduction of selenate or by the addition of pure SeIV derivatives (selenite and selenious acid) led to a concentration-dependent inhibition of PTP activity (Fig. 5). As for glutathione peroxidase activity (cf. Section 4.1), a possible explanation for this observation that free SeIV compounds act as the actual inhibitors of PTPs could be derived from the differences in the metabolism of selenate and selenite in vivo (Fig. 1).

In mammals, selenate is absorbed unmodified by a sodium-dependent cotransport system, which is also involved in sulphate absorption [10]. Furthermore, there is evidence that selenate is distributed unmodified to peripheral tissues, where it is stepwise reduced to the oxidation state −II (Fig. 1). The exact effect of selenate

metabolism in mammalian tissues is not clear yet [14]. Either selenate is metabolised in a similar manner to sulfate or it undergoes reduction during which the oxidation state +IV is formed as an intermediate. Due to the reduction of PTP activity observed in selenate-treated mice, the latter mentioned pathway seems to play an important role.

In contrast to selenate, most of the selenite does not reach the peripheral tissues in the oxidation state +IV since selenite forms selenotrisulfides (oxidation state: −I) during its intestinal absorption. These selenotrisulfides are distributed to organs on the periphery and undergo reduction to the oxidation state −II, from which they can be utilized for the synthesis of functional selenoproteins [10,13]. This hypothesis is supported by the results from the in vitro inhibition test. When selenite and GSH were converted to selenotrisulfides prior to their use in the in vitro inhibition test, the inhibition of PTPs decreased significantly. The remaining inhibition may have derived from a not fully completed synthesis of selenotrisulfides in the model investigated. This must be examined in future investigations with purified selenotrisulfides and pure preparations of PTP1B. The precise inhibition mechanism of SeIV compounds on PTPs in general and on PTP1B in particular seems to be an interesting subject for future investigations using mass spectrometry.

In conclusion, our results on PTP activity and expression can be interpreted as shown in Fig. 8.

High supranutritional selenium doses effect a shift in the glutathione–redox system to a more oxidized state. An enhanced glutathionylation of PTPs is presumably the stimulus for an increase in gene expression.

In the case of very high selenate doses, the inhibitory effect of intermediary selenate metabolites compensates for the increased expression, which, in turn, leads to a correction of insulin signalling and particular changes in the intermediary glucose metabolism. In particular, a reduction of the activity and the expression of gluconeogenic marker enzymes was obtained (Fig. 8). In prior studies with type I diabetic rats, the regulatory effect of selenate on glycolysis and gluconeogenesis was attributed to an increase in the phosphorylation of single components of the insulin signalling pathway. From our present results, we now conclude that the inhibition of PTPs is the cause of the modification of insulin signalling.

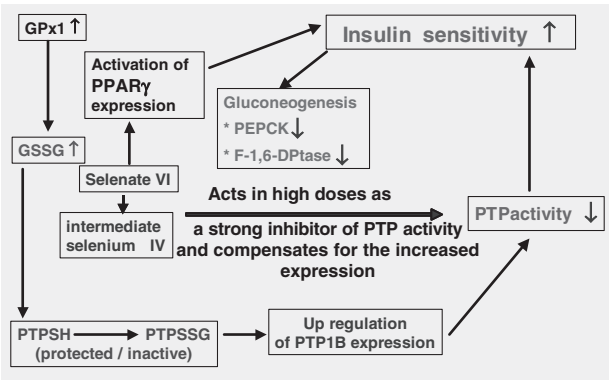

Fig. 8. Possible links between the selenium-dependent redox system, the regulation of PTPs and the resulting influence on glucose metabolism.

Future investigations into the precise regulation of PTP1B mRNA expression and PTP1B protein expression should focus on the role of cellular redox status during these processes.

4.3. Influence on fatty acid metabolism

With regard to fatty acid metabolism, supranutritional selenate led to a significant decrease in plasma cholesterol and triglycerides. Concomitantly, a significant increase in total liver lipid concentration, liver triglyceride concentration and expression of PPARγ was measured.

The main functions of PPARγ consist of adipocyte differentiation and the redistribution of adipose tissue. Furthermore, PPARγ seems to be involved in the distribution of body fat stores. These hypotheses were confirmed by a study with transgenic mice with an ablation of liver PPARγ but with adipose tissues. However, these animals developed fat intolerance, increased adiposity, hyperlipidemia and insulin resistance. It could be concluded that liver PPARγ regulates triglyceride homeostasis, contributing to hepatic steatosis, but protecting other tissues from triglyceride accumulation and insulin resistance [32,33]. Results of other trials in which *db/db* mice were long-term treated with thiazolidinediones showed that these insulin-sensitising pharmaceuticals induced liver PPARγ and its target genes (adipocyte FABP) [34], finally resulting in hepatic steatosis [35,36].

Our study shows that a similar mechanism seems to be activated by selenate. Selenate-treated *db/db* mice gained far less body weight than their selenium-deficient and selenite-treated companions [29]; they showed reduced plasma lipids and a distinct increase in liver lipids. The lipid fractions per gram of total lipids indicate that in selenate-treated *db/db* mice the “rest” to 1 g of total lipids is significantly higher than in the two other groups and therefore demonstrate a higher amount of nonesterified fatty acids. These nonesterified fatty acids in turn can act as natural ligands of PPARγ and therefore contribute to an increase in whole-body insulin sensitivity (Fig. 8).

5. Conclusion

The results of our study with type II diabetic *db/db* mice give some new insight into the mechanisms by which the administration of supranutritional selenate can influence diabetes and insulin resistance. One mechanism of interest is the inhibition of PTPs by intermediary selenate metabolites. This aspect of an antidiabetic action is closely linked to selenium metabolism, since selenium metabolites in the oxidation state +IV are the actual inhibitors of PTPs and they can be generated only from the stepwise

reduction of selenate. This is likewise the reason why selenite fails to develop strong antidiabetic properties, because this selenium compound enters peripheral organs in the selenotrisulfide oxidation state −I. Furthermore, we could demonstrate that the system of PPARs is also initiated by supranutritional selenate. The increased expression of liver PPARγ presumably led to a redistribution of whole-body lipid stores resulting in an increase in liver lipids. In turn, the concentration of lipids in the liver can provide natural ligands of PPARγ and therefore contribute to the increase in insulin sensitivity.

Acknowledgment

We thank Dipl. Biol. Sandra Schneider and Prof. Dr. R. Schmidt from the Biotechnical Centre of Giessen University for their advice in the RT-PCR experiments. Further thanks are addressed to our Bachelor and Masteral students Linda Minke and Jenny Schaefer for their help with analyses within the scope of their Bachelor and Masteral theses.

For financial support, we thank the H.W. Schaumann Foundation for Agricultural Sciences (Hamburg, Germany).

References

[1] NRC (National Research Council). Nutrient requirements of laboratory animals. 4th revised ed. Washington (DC): National Academy Press; 1995.
[2] NRC (National Research Council). Nutrient requirements of poultry. 9th revised ed. Washington (DC): National Academy Press; 1994.
[3] NRC (National Research Council). Nutrient requirements of sheep. 6th revised ed. Washington (DC): National Academy Press; 1995.
[4] NRC (National Research Council). Nutrient requirements of swine. 10th revised ed. Washington (DC): National Academy Press; 1998.
[5] NIH (National Institute of Health) (Updated: 08/01/2004): http://ods.od.nih.gov/factsheets/selenium.asp.
[6] Brigelius-Flohé R. Tissue-specific functions of individual glutathione peroxidases. Free Radic Biol Med 2000;27:951–65.
[7] Köhrle J. Thyroid hormone deiodinases — a selenoenzyme family acting as gate keepers to thyroid hormone action. Acta Med Austriaca 1996;23:17–30.
[8] May JM, Mendiratta S, Hill KE, Burk RF. Reduction of dehydroascorbate to ascorbate by the selenoenzyme thioredoxin reductase. J Biol Chem 1997;272:22607–10.
[9] Wolffram S, Berger B, Grenacher B, Scharrer E. Transport of selenoamino acids and their sulfur analogues across the intestinal brush border membrane of pigs. J Nutr 1989;119:706–12.
[10] Wolffram S, Arduser F, Scharrer E. In vivo intestinal absorption of selenate and selenite by rats. J Nutr 1985;115:454–9.
[11] Beilstein MA, Whanger PD. Chemical forms of selenium in rat tissues after administration of selenite or selenomethionine. J Nutr 1986; 116:1711–9.
[12] Beilstein MA, Whanger PD. Deposition of dietary organic and inorganic selenium in rat erythrocyte proteins. J Nutr 1986;116:1701–10.
[13] Suzuki KT, Shiobara Y, Itoh M, Omichi M. Selective uptake of selenite by red blood cells. Analyst 1998;123:63–7.
[14] Shiobara Y, Ogra Y, Suzuki KT. Speciation of metabolites of selenate in rats by HPLC-ICP-MS. Analyst 1999;124:1237–41.
[15] Sunde RA, Evenson JK. Serine incorporation into the selenocysteine moiety of glutathione peroxidase. J Biol Chem 1997;262:933–7.
[16] Böck A, Forchhammer K, Heider J, Leinfelder W, Sawers G, Veprek B, et al. Selenocysteine: the 21st amino acid. Mol Microbiol 1991; 5:515–20.
[17] Park SI, Park JM, Chittum HS, Yang ES, Carlson BA, Lee BJ, et al. Selenocysteine tRNAs as central components of selenoprotein biosynthesis in eukaryotes. Biomed Environ Sci 1997;10:116–24.
[18] Ezaki O. The insulin-like effect of selenate in rat adipocytes. J Biol Chem 1990;262:6658–62.
[19] Furnsinn C, Englisch R, Ebner K, Nowotny P, Vogle C, Waldhausl W. Insulin-like vs. non-insulin stimulation of glucose metabolism by vanadium tungsten and selenium compounds in rat muscle. Life Sci 1996;59:1989–2000.
[20] McNeill JH, Delgatty HL, Battell ML. Insulinlike effects of sodium selenate in streptozotocin-induced diabetic rats. Diabetes 1991;40: 1675–8.
[21] Battell ML, Delgatty HL, McNeill JH. Sodium selenate corrects glucose tolerance and heart function in STZ diabetic rats. Mol Cell Biochem 1998;179:27–34.
[22] Berg EA, Wu JY, Campbell L, Kagey M, Stapleton SR. Insulin-like effects of vanadate and selenate on the expression of glucose-6-phosphate dehydrogenase and fatty acid synthase in diabetic rats. Biochimie 1995;77:919–24.
[23] Stapleton SR, Jivraj S, Wagle A. Insulin and the insulin-mimetic selenium mediate the regulation of glucose-6-phosphate-dehydrogenase gene expression via different signal proteins. FASEB J 1998; 12:1404.
[24] Becker DJ, Reul B, Ozcelikay AT, Buchet JP, Henquin JC, Brichard SM. Oral selenate improves glucose homeostasis and partly reverses abnormal expression of liver glycolytic and gluconeogenic enzymes in diabetic rats. Diabetologia 1996;39:3–11.
[25] Stapleton SR, Garlock GL, Foellmi-Adams L, Kletzien RE. Selenium potent stimulator of tyrosyl phosphorylation and activator of MAP kinase. Biochim Biophys Acta 1997;1355:259–69.
[26] Hei YJ, Farahbakshian S, Chen X, Battel ML, McNeill JH. Stimulation of MAP kinase and S6 kinase by vanadium and selenium in rat adipocytes. Mol Cell Biochem 1998;178:367–75.
[27] Sheng XQ, Huang KX, Xu HB. New experimental observation on the relationship of selenium and diabetes. Biol Trace Elem Res 2004; 99:241–53.
[28] Mueller AS, Pallauf J, Rafael J. The chemical form of selenium affects insulinomimetic properties of the trace element: investigations in type II diabetic *dbdb* mice. J Nutr Biochem 2003;14:637–47.
[29] Mueller AS, Most E, Pallauf J. Effects of a supranutritional dose of selenate compared to selenite on insulin sensitivity in type II diabetic *dbdb* mice. J Anim Physiol Anim Nutr 2005;89:94–104.
[30] Ferre P. The biology of peroxisome proliferator-activated receptors. Relationship with lipid metabolism and insulin sensitivity. Diabetes 2004;53:S43–S50.
[31] Vidal-Puig A, Jimenez-Linan M, Lowell BB, Hamann A, Hu E, Spiegelman B, et al. Regulation of PPARγ gene expression by nutrition and obesity in rodents. J Clin Invest 1996;97:2553–61.
[32] Schadlinger SE, Bucher NE, Schreiber BM, Farmer SR. PPARγ2 regulates lipogenesis and lipid accumulation in steatotic hepatocytes. Am J Physiol Endocrinol Metab 2005;288:E1195–205.
[33] Gavrilova O, Haluzik M, Matsusue K, Cutson JJ, Johnson L, Dietz KR, et al. Liver peroxisome proliferator-activated receptor γ contributes to hepatic steatosis, triglyceride clearance, and the regulation of body fat mass. J Biol Chem 2003;278:34268–76.
[34] Memon RA, Tecott LH, Nonogaki K, Beigneux A, Moser AH, et al. Upregulation of peroxisome proliferator activated receptors (PPAR-alpha) and PPAR-gamma messenger ribonucleic acid expression in the liver in murine obesity: troglitazone induces expression of PPAR-gamma-responsive adipose tissue specific genes in the liver of obese diabetic mice. Endocrinology 2000;141:4021–31.
[35] Burant CF, Sreenan S, Hirano K-I, Tai TAC, Lohmiller J, et al. Troglitazone action is independent of adipose tissue. J Clin Invest 1997;100:2900–8.

[36] Chao L, Marcus-Samuels B, Mason MM, Moitra J, Vinson C, et al. Adipose tissue is required for the antidiabetic, but not for the hypolipidemic, effect of thiazolidinediones. J Clin Invest 2000;106: 1221–8.
[37] Tappel ME, Chaudiere J, Tappel AL. Glutathione peroxidase activities of animal tissues. Comp Biochem Physiol 1982;73 [B]:945–9.
[38] Cohen MB, Duvel DL. Characterization of the inhibition of glutathione reductase and the recovery of enzyme activity in exponentially growing murine leukemia (L1210) cells treated with 1,3-bis(2-chloroethyl)-1-nitrosourea. Biochem Pharmacol 1988;37: 3317–20.
[39] Griffith OW. Determination of glutathione and glutathione disulfide using glutathione reductase and 2-vinylpyridine. Anal Biochem 1982; 106:207–12.
[40] Gromer S, Arscott LD, Williams CH, Schirmer RH, Becker K. Human placenta thioredoxin reductase. Isolation of the selenoenzyme, steady state kinetics, and inhibition by therapeutic gold compounds. J Biol Chem 1998;273:20096–101.
[41] Zhu L, Goldstein B. Use of an anaerobic chamber environment for the assay of endogenous cellular protein tyrosine phosphatase activities. Biol Proced Online 2002;4:1–9.
[42] Montalibet J, Skorey KI, Kennedy BP. Protein tyrosine phosphatase: enzymatic assays. Methods 2005;35:2–8.
[43] Ganther HE. Selenotrisulfides. Formation by the reaction of thiols with selenious acid. Biochemistry 1968;7:2898–905.
[44] Chomczynski P, Sacchi N. Single step method of RNA isolation by acid guanidiniumthiocyanate–phenol–chloroform extraction. Anal Biochem 1987;162:156–9.
[45] Pontremoli P, Melloni E. Fructose-1.6-diphosphatase from rabbit liver. Methods Enzymol 1975;42:354–9.
[46] Warren GB, Tipton KF. Pig liver pyruvate carboxylase. Purification, properties and cation specificity. Biochem J 1976;139:297–310.
[47] Wimonwatwatee T, Heydari AR, Wu WT, Richardson A. Effect of age on the expression of phosphoenolpyruvate carboxykinase in rat liver. Am J Physiol Gastrointest Liver Physiol 1994;267: G201–4.
[48] Bradford MM. A rapid sensitive method for the quantitation of microgram quantities of protein utilizing the principle of protein-dye binding. Anal Biochem 1976;72:248–54.
[49] Thompson HJ, Ip C. Temporal changes in tissue glutathione in response to chemical form, dose, and duration of selenium treatment. Relevance to cancer chemoprevention by selenium. Biol Trace Elem Res 1991;30:163–73.
[50] Hoffmann DJ, Heinz GH, LeCaptain LJ, Eisemann JD, Pendleton GW. Toxicity and oxidative stress of different forms of organic selenium and dietary protein in mallard ducklings. Arch Environ Contam Toxicol 1996;31:120–7.
[51] Schäfer K, Kyriakopoulos A, Gessner H, Grune T. Effects of selenium deficiency on fatty acid metabolism in rats fed fish oil-enriched diets. J Trace Elem Med Biol 2004;18:89–97.
[52] Khamaisi M, Kavel O, Rosenstock M, Porat M, Yuli M, Kaiser N, et al. Effect of inhibition of glutathione synthesis on insulin action: in vivo and in vitro studies using buthionine sulfoximine. Biochem J 2000;349(Pt 2):579–86.
[53] Cho KJ, Moini H, Shon HK, Chung AS, Packer L. Alpha-lipoic acid decreases thiol reactivity of the insulin receptor and protein tyrosine phosphatase 1B in 3T3-L1 adipocytes. Biochem Pharmacol 2003;66: 849–58.
[54] Lu B, Ennis D, Lai R, Bogdanovic E, Nikolov R, Salamon L, et al. Enhanced sensitivity of insulin-resistant adipocytes to vanadate is associated with oxidative stress and decreased reduction of vanadate (+5) to vanadyl (+4). J Biol Chem 2001;276(38):35589–98.
[55] Denu JM, Dixon JE. Protein tyrosine phosphatases: mechanisms of catalysis and regulation. Curr Opin Chem Biol 1998;2:633–41.
[56] Zinker BA, Rondinone CM, Trevillyan JM, Gum RJ, Clampit JE, Waring JF, et al. PTP1B antisense oligonucleotide lowers PTP1B protein, normalizes blood glucose, and improves insulin sensitivity in diabetic mice. Proc Natl Acad Sci U S A 2002;99:11357–62.
[57] Gum RJ, Gaede LL, Koterski SL, Heindel M, Clampit JE, Zinker BA, et al. Reduction of protein tyrosine phosphatase 1B increases insulin-dependent signaling in *ob/ob* mice. Diabetes 2003;52:21–8.
[58] Ramachandran C, Kennedy BP. Protein tyrosine phosphatase 1B: a novel target for type 2 diabetes and obesity. Curr Top Med Chem 2003;3:749–57.
[59] Harley EA, Levens N. Protein tyrosine phosphatase 1B inhibitors for the treatment of type 2 diabetes and obesity: recent advances. Curr Opin Investig Drugs 2003;4:1179–89.
[60] Salmeen A, Andersen JN, Myers MP, Meng TZ, Hinks JA, Tonks NK, et al. Redox regulation of protein tyrosine phosphatase 1B involves a sulphenyl-amide intermediate. Nature 2003;423:769–73.
[61] Van Montfort RL, Congreve M, Tisi D, Carr R, Jhoti H. Oxidation state of the active-site cysteine in protein tyrosine phosphatase 1B. Nature 2003;423:773–7.
[62] Barrett WC, DeGnore JP, Koenig S, Fales HM, Keng YF, Zhang ZY, et al. Regulation of PTP1B via glutathionylation of the active site cysteine 215. Biochemistry 1999;28:6699–705.
[63] Mahadev K, Zilbering A, Zhu L, Goldstein BJ. Insulin-stimulated hydrogen peroxide reversibly inhibits protein-tyrosine phosphatase 1B in vivo and enhances the early insulin action cascade. J Biol Chem 2001;276:21938–42.
[64] McClung JP, Ronecker CA, Weipeng M, Lisk DJ, Langlais P, Liu F, et al. Development of insulin resistance and obesity in mice overexpressing cellular glutathione peroxidase. Proc Natl Acad Sci U S A 2004;101:8852–7.